Interface crack between isotropic Kirchhoff plates

András Szekrényes

Meccanica
An International Journal of Theoretical and Applied Mechanics AIMETA

ISSN 0025-6455

Meccanica
DOI 10.1007/s11012-012-9611-9

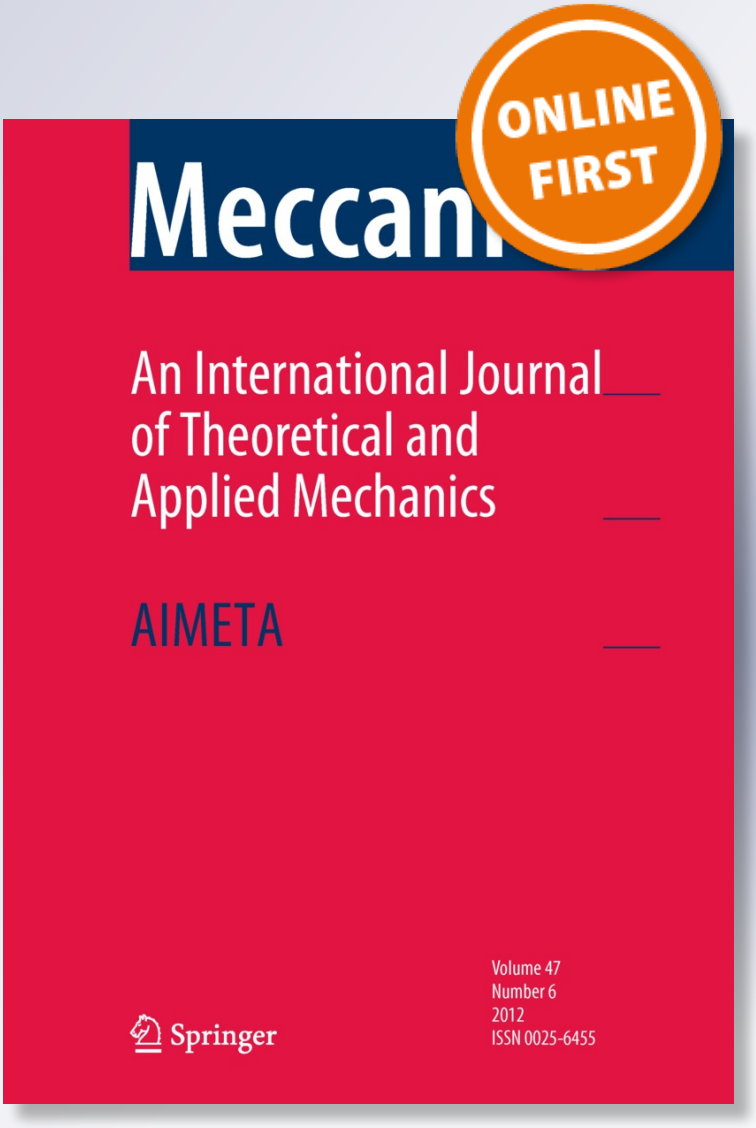

Springer

Meccanica
DOI 10.1007/s11012-012-9611-9

Interface crack between isotropic Kirchhoff plates

András Szekrényes

Received: 6 March 2012 / Accepted: 14 September 2012

Abstract In this work Kirchhoff plate theory is used to calculate the energy release rate function in delaminated isotropic plates. The approximation is based on the consideration of the equilibrium equations and the displacement continuity between the interface plane of a double-plate model. It is shown that the interface shear stresses are governed by a fourth order partial differential equation system. As an example, a simply supported delaminated plate subjected to a point force is analyzed adopting Lévy plate formulation and the mode-II and mode-III energy release rate distributions along the crack front were calculated by the J-integral. To confirm the analytical results the 3D finite element model of the delaminated plate was created, the energy release rates were calculated by the virtual crack-closure technique and the J-integral. The results indicate a good agreement between analysis and numerical computation.

Keywords Fracture mechanics · Delamination · Interface fracture · Mixed-mode II/III fracture · Plate theory

A. Szekrényes (✉)
Department of Applied Mechanics, Budapest University of Technology and Economics, Műegyetem rkp. 5, 1111 Budapest, Hungary
e-mail: szeki@mm.bme.hu

1 Introduction

Kirchhoff plate theory plays a very significant role in the mechanical design of engineering structures such as metal [1–3], composite [4] and sandwich [5] structures. One of the damage modes of these engineering materials is the formation of cracks and delamination surfaces. The energy release rate (ERR) is an important parameter in fracture mechanics to characterize the fracture properties of metals, plastics, composites and other engineering materials [6]. In general the interlaminar fracture is investigated by beam specimens including relatively simple loading conditions and geometry. Generally, simple beam theory is applied for the analytical description of these systems including mode-I (opening mode), [7–12] mode-II (sliding mode) [8, 13–15] and mode-III (tearing mode) fracture conditions [16–19]. At the same time, numerous refined models were developed (e.g.: [20–28]).

Under mixed-mode conditions (I/II (e.g.: [25, 29–31]), I/III (e.g.: [32, 33]), II/III ([34–39]) or I/II/III [19, 40, 41]) the mode partitioning is an important issue. In this respect Williams [42] provided a simple beam theory based (global) method for the separation of energy release rates under mixed-mode I/II condition. However, only simple loading schemes were considered and the method gave misleading result for unsymmetric specimens. Suo and Hutchinson [43, 44] developed the so-called local mode decomposition method. The energy release rate was calculated by beam theory, the mode mixity was resolved by a continuum

Published online: 09 October 2012

model based on integral equation methods. Independently, Davidson et al. [45] proposed the crack tip element (CTE) analysis, where—similarly to [43]—the energy release rate was calculated by beam theory, but the mode ratio was obtained by finite element analysis. Both methods gave realistic results for unsymmetrically delaminated systems.

The J-integral was developed by Rice [46] and Cherepanov [47] independently, first for 2D problems, later it was generalized for 3D problems too [48–50]. For plate bending problems including surface or edge cracks the J-integral—among others—was applied by Valaire et al. [51] and Wearing et al. [52]. For delaminated plates, where the crack lies in the midplane of the plate the J-integral was used by Lee and Tu [53]. The problem under consideration was an edge-delaminated plate subjected to pure bending and/or uniaxial tension which involves relatively simple solution procedure. Later Wang and Huang [54] proposed the continuous analysis of delaminated plates based on Fourier series solution. The problem of embedded delaminations was analyzed.

Continuing with plate problems, Bruno and Greco [55] performed the refined analysis of cracked composite plates including interface analysis, where the interface stiffness was considered to tend to infinity. Although in that work a plate analysis was referred to, in fact only simple (beam-like) loading schemes were adopted. Later their model was completed with the effect of transverse shear [56]. They applied a similar scheme to that Williams provided for mode partitioning in mixed-mode I/II cases.

The classical work of Suo and Hutchinson inspired Wang and Qiao [57] to improve the so-called local method by transverse shear effect and modify the equations for bi-material beams too. It was a closed-form solution, however due to the high number of complex equations it requires much computation. Later the method was further developed by completing the model by a flexible joint at the crack tip [22]. Essentially, the interface shear and normal (or peel) stresses were captured and the displacement continuity of the interface was formulated. The method was developed to analyze mixed-mode I/II problems only.

Nowadays more and more attention is favored to the mode-III and mixed-mode II/III or I/III fracture of composite materials. Recently, de Morais and Pereira published many studies for carbon/epoxy systems involving the bending of plate specimens. The mode-III 4-point bending plate [17], the mixed-mode I/III 8-point bending [33] and the mixed-mode II/III 6-point bending plate [39] specimens involve the bending of delaminated plates.

Apart from the virtual crack-closure technique (VCCT) (e.g.: [40, 58]), there are only few alternatives for the possible fracture mechanical analysis of these plate bending systems. The method of Qiao and Wang [59] applies only for beam-like geometry, however the basic equations for a possible plate analysis were summarized [60]. As another alternative Sankar and Sonik [61] and Davidson et al. [62] published plate theory based methods in conjunction with finite element analysis. The energy release rates (mode-I, mode-II and mode-III) were calculated by using the classical plate theory (CPT) forces and moments, strains and midplane curvatures, respectively, however all of these were calculated by shell finite element models. A very good agreement with 3D FE analysis (VCCT) was obtained. The so-called crack-tip force method (CTFM) [63] applies the nodal forces for the ERR calculation. It gives almost the same results as the VCCT. Later, a 3D modelling technique was developed based on interface and first order shear deformable plate theory [64]. The method was effective, however finite element implementation of the equations is necessary. This short overview shows that a purely analytical solution is not available for general plate bending problems including through the width delamination surfaces.

In this report it is shown how Kirchhoff plate theory can be used to predict the energy release rate distribution in bent plate specimens under mixed-mode II/III loading conditions. Although the present formulation applies material isotropy, it is applicable for quasi-isotropic and short random-fiber reinforced composite laminates or polymer materials. First, the undelaminated part of the plate is treated as a double-plate system by formulating the proper kinematic continuity conditions over the interface. Then, the governing equations of the interface shear stress field are developed. As an example a simply supported, isotropic, symmetrically delaminated plate is analyzed. The function of the mode-II and mode-III ERRs is determined and the results are compared to a 3D FE model evaluated by the VCCT and the J-integral.

2 Kirchhoff plate model, undelaminated region

Let us consider the differential plate elements in Fig. 1, which are the top and bottom layers of the uncracked part of a plate containing a delamination. The thickness of the elements is t. The in-plane force equilibrium of the top plate element in the x and y direction, respectively involves:

$$\begin{aligned} \frac{\partial N_x}{\partial x} - \frac{\partial N_{xy}}{\partial y} &= \tau_{xz} \\ -\frac{\partial N_{xy}}{\partial x} + \frac{\partial N_y}{\partial y} &= \tau_{yz} \end{aligned} \tag{1}$$

where N_x, N_y are the in-plane normal forces, N_{xy} is the in-plane shear force, $\tau_{xz} = \tau_{xz}(x, y)$ and $\tau_{yz} = \tau_{yz}(x, y)$ are the interface shear stress in the x and y directions. Second, we consider the moment equilibrium about axes x and y resulting in:

$$\begin{aligned} \frac{\partial M_x}{\partial x} + \frac{\partial M_{xy}}{\partial y} &= -\tau_{xz}\frac{t}{2} \\ \frac{\partial M_{xy}}{\partial x} + \frac{\partial M_y}{\partial y} &= -\tau_{yz}\frac{t}{2} \end{aligned} \tag{2}$$

where M_x, M_y and M_{xy} are the bending and twisting moments, respectively. We note that the peel stress, σ_z is not considered in the present analysis. To involve the interface peel stress the consideration of the shear forces (Q_x and Q_y) in Eqs. (5)–(8) would be necessary (see also the force equilibrium in z by Fig. 1). However in this case Kirchhoff plate theory is not applicable, because together with the shear forces we have too many parameters and more constitutive equations are required. Therefore, the peel stress is not taken into account here, due to the fact that in this case plate theory with transverse shear effect must be used. The present formulation is suitable to analyze mixed-mode II/III problems only. Following the basic equations of Kirchhoff plate theory the moment-curvature and the twisting moment-twisting curvature relationships, respectively still hold [1–4]:

$$\begin{aligned} M_x &= -I_1 E_1 (w_{,xx} + \nu w_{,yy}) \\ M_y &= -I_1 E_1 (w_{,yy} + \nu w_{,xx}) \\ M_{xy} &= M_{yx} = -I_1 E_1 (1-\nu) w_{,xy} \end{aligned} \tag{3}$$

where $I_1 = 1/3 \cdot t^3$ is the area moment of inertia of one plate element with thickness of t and with a reference

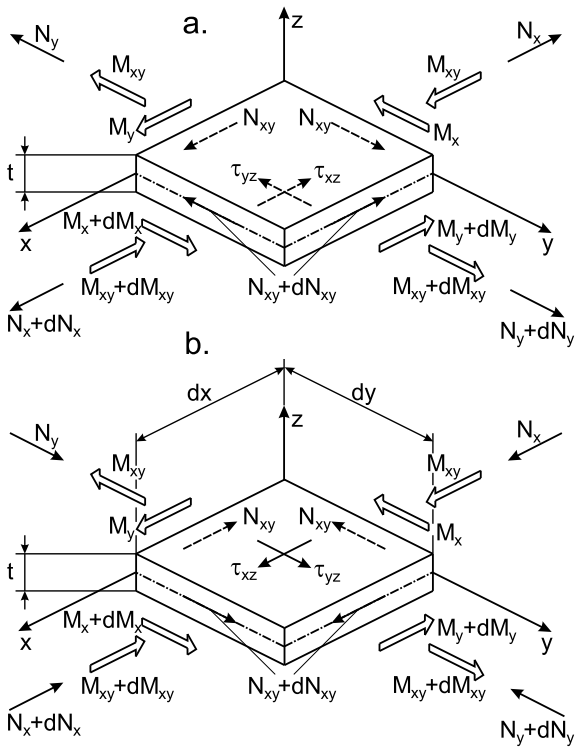

Fig. 1 Equilibrium of the *top* (**a**) and *bottom* (**b**) differential plate elements

located at the interface plane, and $E_1 = E/(1-\nu^2)$. Due to the midplane delamination the deflection of the top and bottom plate elements is the same, i.e.: $w_1 = w_2 = w$. Assuming plane stress state, the general relationship between in-plane forces and strains for isotropic plates in matrix form becomes [1]:

$$\begin{bmatrix} N_x \\ N_y \\ N_{xy} \end{bmatrix} = E_1 \begin{bmatrix} 1 & \upsilon & 0 \\ \upsilon & 1 & 0 \\ 0 & 0 & (1-\upsilon)/2 \end{bmatrix} \begin{bmatrix} \varepsilon_x^0 \\ \varepsilon_y^0 \\ \gamma_{xy}^0 \end{bmatrix} \tag{4}$$

Expressing the in-plane strains in terms of the in-plane displacement components we have:

$$\begin{aligned} \varepsilon_x^0 &= \frac{\partial u_0}{\partial x} = \frac{1}{Et}(N_x - \upsilon N_y), \qquad \gamma_{xy}^0 = \frac{N_{xy}}{Gt} \\ \varepsilon_y^0 &= \frac{\partial v_0}{\partial x} = \frac{1}{Et}(N_y - \upsilon N_x) \end{aligned} \tag{5}$$

The next step is the formulation of the kinematic continuity conditions over the interface of the uncracked portion of a delaminated plate system, where the top and bottom plates are connected to each other. Here we

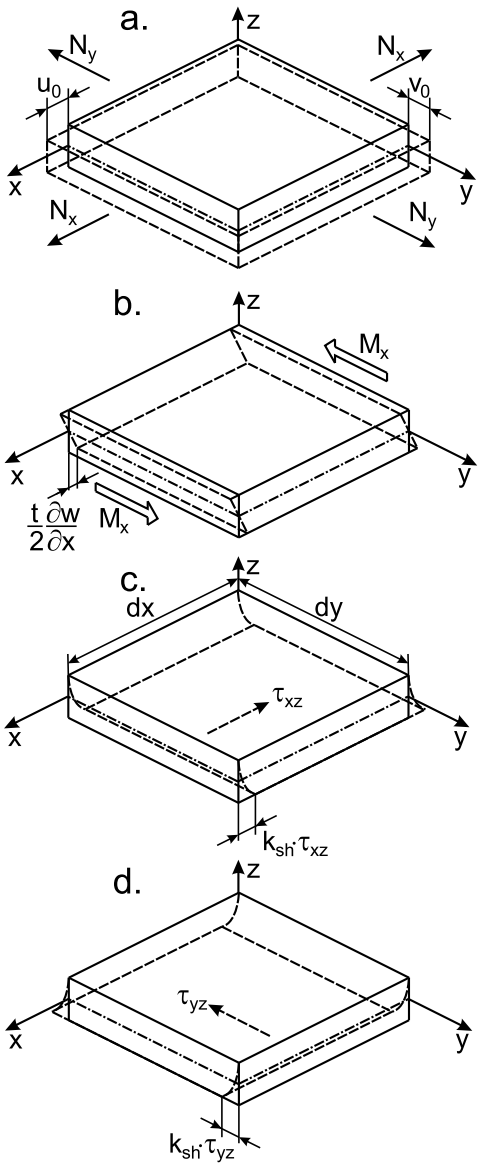

Fig. 2 Deformations of the *top* plate element under in-plane forces (**a**), bending (**b**) and interface shear stresses (**c**), (**d**)

consider the simplest case, namely when the plate is symmetrically delaminated. Figure 2 presents the possible sources of the in-plane displacements: in-plane forces (a), bending (b) (both about axes x and y) and finally the interface shear deformation (c and d). The resultant displacement from these effects are:

$$u_i = \pm\left\{\frac{1}{Et}\int\left(N_x^{(i)} - \upsilon N_y^{(i)}\right)dx + z\frac{\partial w_i}{\partial x} - k_{sh}\tau_{xz}^{(i)}(x,y,z)\right\} \tag{6}$$

$$v_i = \pm\left\{\frac{1}{Et}\int\left(N_y^{(i)} - \upsilon N_x^{(i)}\right)dy + z\frac{\partial w_i}{\partial y} - k_{sh}\tau_{yz}^{(i)}(x,y,z)\right\}$$

where the upper sign and $i = 1$ goes with the top plate element, the lower sign and $i = 2$ goes with the bottom plate element, moreover $k_{sh} = t/3G$ is the shear compliance for isotropic material [65]. The shear stresses are [1]:

$$\begin{aligned}\tau_{xz}^{(i)}(x,y,z) &= \tau_{xz}(x,y)\left(1 - \frac{(z \pm t/2)^2}{t^2}\right)\\ \tau_{yz}^{(i)}(x,y,z) &= \tau_{yz}(x,y)\left(1 - \frac{(z \pm t/2)^2}{t^2}\right)\end{aligned} \tag{7}$$

With respect to the shear strain three effects should be considered as it is shown by Fig. 3 [66]: in-plane shear force (a), twisting moment (b) and the shear strain induced by interface shear stresses (c):

$$\gamma_{xy}^{(i)} = \pm\left\{-\frac{N_{xy}^{(i)}}{Gt} + 2z\frac{\partial^2 w_i}{\partial x \partial y} - k_{sh}\left(\frac{\partial \tau_{xz}^{(i)}(x,y,z)}{\partial y} + \frac{\partial \tau_{yz}^{(i)}(x,y,z)}{\partial x}\right)\right\} \tag{8}$$

To satisfy the continuity conditions the in-plane displacements and the shear strain at the interface must be zero. Therefore, based on Eqs. (6) the conditions for the in-plane displacements formulated in the local x, y, z coordinate system of the top plate element are:

$$\begin{aligned}u_1|_{z=-t/2} &= \frac{1}{Et}\int(N_x - \upsilon N_y)dx - \frac{t}{2}\frac{\partial w}{\partial x} - k_{sh}\tau_{xz} = 0\\ v_1|_{z=-t/2} &= \frac{1}{Et}\int(N_y - \upsilon N_x)dy - \frac{t}{2}\frac{\partial w}{\partial y} - k_{sh}\tau_{yz} = 0\end{aligned} \tag{9}$$

The superscript (i) is omitted in the equations above because we obtain the same for the bottom plate element due to the symmetric delamination. Similarly to u and v, the shear strain must be zero at the interface due to the opposite deformation of the top and bottom

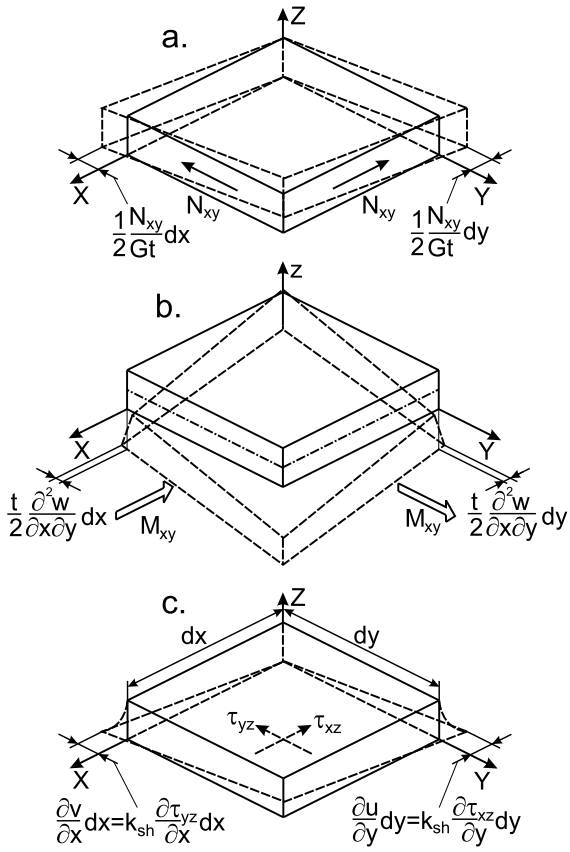

Fig. 3 Deformations of the *top* plate element under in-plane shear force (**a**), torsion (**b**) and interface shear stresses (**c**)

plate elements, i.e.:

$$\gamma_{xy}^{(1)}\big|_{z=-t/2} = -\frac{N_{xy}}{Gt} - t\frac{\partial^2 w}{\partial x\partial y} - k_{sh}\left(\frac{\partial \tau_{xz}}{\partial y} + \frac{\partial \tau_{yz}}{\partial x}\right) = 0 \tag{10}$$

These equations can be obtained also by formulating the conditions for the bottom plate element. We note that Wang and Qiao derived only one of these conditions, first for a symmetrically delaminated end-notched flexure (ENF) specimen [22] and second for a 2D beam problem [59].

The basic equations for the uncracked portion of delaminated Kirchhoff plates are given by Eqs. (1), (2) (equilibrium equations), (3) (moment-curvature relationships), (9) and (10) (kinematic conditions), which are totally ten equations building a system of partial differential equations. The ten parameters are: N_x, N_y, N_{xy}, M_x, M_y, M_{xy}, τ_{xz}, τ_{yz}, $\partial w/\partial x$ and $\partial w/\partial y$. Utilizing the moment-curvature equations (Eqs. (3) and taking them back into Eq. (2)) it is possible to obtain the governing differential equation of the plate deflection for the uncracked region in the form of:

$$\frac{\partial^4 w}{\partial x^4} + 2\frac{\partial^4 w}{\partial x^2\partial y^2} + \frac{\partial^4 w}{\partial y^4} = \frac{t}{2I_1E_1}\left(\frac{\partial \tau_{xz}}{\partial x} + \frac{\partial \tau_{yz}}{\partial y}\right) \tag{11}$$

i.e., the inhomogeneity is caused by the interface shear stresses. Consequently, Eq. (11) can be solved only if we know the functions of the interface stresses, $\tau_{xz}(x, y)$ and $\tau_{yz}(x, y)$. The solutions can be obtained by solving partial differential equations detailed in next section. In order to obtain a compatible displacement field the following condition for the in-plane displacements and the shear strain should be satisfied [66]:

$$\gamma_{xy}^{(1)}\big|_{z=-t/2} = \frac{\partial u_1}{\partial y} + \frac{\partial v_1}{\partial x}\bigg|_{z=-t/2} \tag{12}$$

It can be seen that the second and third terms in Eq. (9) satisfy automatically the compatibility equation. On the contrary, the first terms in the same equations must be investigated. Differentiating the first terms in Eqs. (9) and (10) with respect to x and y, respectively and utilizing the compatibility condition we have:

$$\frac{\partial^2 N_{xy}}{\partial x\partial y} = -\frac{1}{2(1+\nu)}\left(\frac{\partial^2 N_x}{\partial y^2} + \frac{\partial^2 N_y}{\partial x^2} - \nu\left\{\frac{\partial^2 N_x}{\partial x^2} + \frac{\partial^2 N_y}{\partial y^2}\right\}\right) \tag{13}$$

Incorporating Eqs. (1) the following PDE is obtained for N_{xy}:

$$-\left\{\frac{\partial^4 N_{xy}}{\partial x^4} + 2\frac{\partial^4 N_{xy}}{\partial x^2\partial y^2} + \frac{\partial^4 N_{xy}}{\partial y^4}\right\} = \frac{\partial^3 \tau_{xz}}{\partial y^3} + \frac{\partial^3 \tau_{yz}}{\partial x^3} - \nu\left\{\frac{\partial^3 \tau_{xz}}{\partial x^2\partial y} + \frac{\partial^3 \tau_{yz}}{\partial x\partial y^2}\right\} \tag{14}$$

which should be incorporated in order to obtain a kinematically compatible displacement field.

3 Governing equations of interface shear stresses

In this section we derive the partial differential equations for the shear stresses, $\tau_{xz}(x, y)$ and $\tau_{yz}(x, y)$.

The first step is that we express $\partial w/\partial x$, $\partial w/\partial y$ and $\partial^2 w/\partial x \partial y$ from Eqs. (9) and (10), respectively. Then we take them back into the moment-curvature equations (Eq. (3)). Finally, the first derivatives of the moments are put into the equilibrium equations (Eq. (2)). This procedure leads to the following equations in terms of $\tau_{xz}(x, y)$ and $\tau_{yz}(x, y)$:

$$\begin{aligned}
&\frac{\partial^2 \tau_{xz}}{\partial x^2} + \frac{(1-\nu)}{2}\frac{\partial^2 \tau_{xz}}{\partial y^2} \\
&\quad + \frac{(1+\nu)}{2}\frac{\partial^2 \tau_{yz}}{\partial x \partial y} - \frac{3(1-\nu)}{8t^2}\tau_{xz} = 0 \\
&\frac{\partial^2 \tau_{yz}}{\partial y^2} + \frac{(1-\nu)}{2}\frac{\partial^2 \tau_{yz}}{\partial x^2} \\
&\quad + \frac{(1+\nu)}{2}\frac{\partial^2 \tau_{xz}}{\partial x \partial y} - \frac{3(1-\nu)}{8t^2}\tau_{yz} = 0
\end{aligned} \tag{15}$$

It is required to separate the equations with respect to $\tau_{xz}(x, y)$ and $\tau_{yz}(x, y)$. Therefore, from the first of Eqs. (15) we express $\partial^2 \tau_{yz}/\partial x \partial y$, $\partial^4 \tau_{yz}/\partial x^3 \partial y$, and $\partial^4 \tau_{yz}/\partial x \partial y^3$. Differentiating the second of Eqs. (15) with respect to x and y and substituting back the former terms, the following equation is obtained:

$$\begin{aligned}
&\frac{\partial^4 \tau_{xz}}{\partial x^4} + \frac{\partial^4 \tau_{xz}}{\partial y^4} - A\left(\frac{\partial^2 \tau_{xz}}{\partial x^2} + \frac{\partial^2 \tau_{xz}}{\partial y^2}\right) \\
&\quad + B\frac{\partial^4 \tau_{xz}}{\partial x^2 \partial y^2} + C\tau_{xz} = 0
\end{aligned} \tag{16}$$

A similar mathematical manipulation of Eq. (15) results in:

$$\begin{aligned}
&\frac{\partial^4 \tau_{yz}}{\partial x^4} + \frac{\partial^4 \tau_{yz}}{\partial y^4} - A\left(\frac{\partial^2 \tau_{yz}}{\partial x^2} + \frac{\partial^2 \tau_{yz}}{\partial y^2}\right) \\
&\quad + B\frac{\partial^4 \tau_{yz}}{\partial x^2 \partial y^2} + C\tau_{yz} = 0
\end{aligned} \tag{17}$$

where:

$$A = \frac{3(3-\nu)}{8t^2}, \qquad B = 2, \qquad C = \frac{9(1-\nu)}{32t^4} \tag{18}$$

i.e., the governing equations of the interface shear stresses are given by fourth order PDEs. In the next section we present the solution for a simply supported plate subjected to point force.

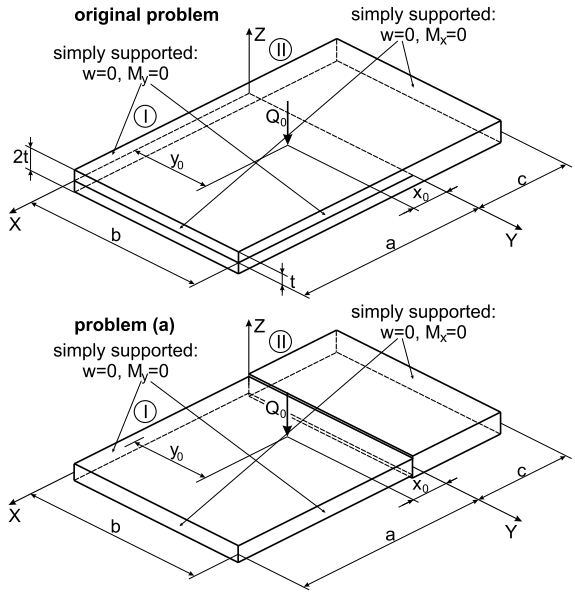

Fig. 4 A simply supported delaminated plate subjected to point force. Subproblem (a): stepped thickness plate

4 Solution of a simply supported delaminated plate

The simply supported boundary conditions for a rectangular plate mean that if $x = a$ or $x = -c$ then $w = 0$, $M_x = 0$, moreover if $y = 0$ or $y = b$ then $w = 0$, $M_y = 0$ as it is given in [4], p. 247. Let us consider now Figs. 4 and 5, where the whole problem is divided into two subproblems: problem (a) and problem (b). Problem (a) in Fig. 4 is a delaminated plate without the consideration of the interface shear stresses. This problem is treated as a general plate bending problem using Kirchhoff plate theory. Problem (b) (Fig. 5) implies that the plate is loaded by the interface shear tractions, $\tau_{xz}(x, y)$ and $\tau_{yz}(x, y)$. This problem is solved by using the equations presented in Sects. 2–3. We calculate the initial values of the unknown shear tractions from problem (a) [20, 67]. This provides an improvement with respect to the original (a) problem.

4.1 Problem (a)—simply supported stepped thickness plate

In fact this problem is treated as a stepped thickness plate [68, 69], where the different bending stiffness of the delaminated and uncracked parts are considered (see Fig. 4). The deflection and the area moment of in-

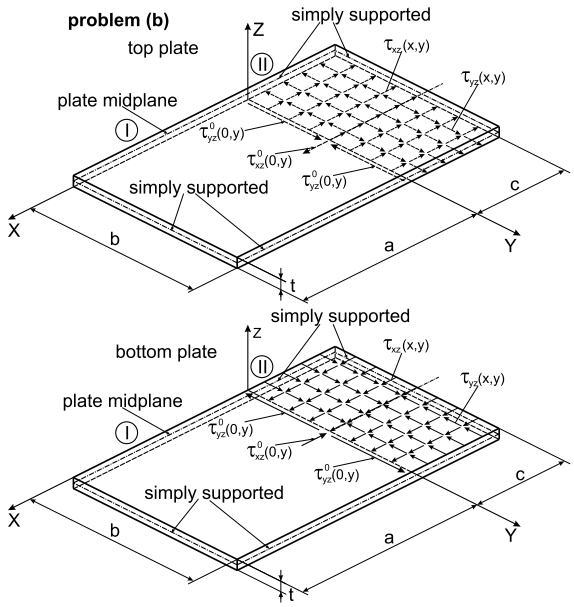

Fig. 5 A simply supported delaminated plate subjected to point force. Subproblem (b): plate subject to shear tractions in the undelaminated region

ertias of the cracked and uncracked plate portions are:

$$\begin{aligned} &w_I^a(x,y): \quad 0 \le x \le a, \quad 0 \le y \le b \\ &I_1^I = \frac{1}{6}t^3 \\ &w_{II}^a(x,y): \quad -c \le x \le 0, \quad 0 \le y \le b \\ &I_1^{II} = \frac{2}{3}t^3 \end{aligned} \tag{19}$$

In accordance with Lévy plate formulation [4], we apply the following solutions:

$$\begin{aligned} w_I^a(x,y) &= \sum_{n=1}^{\infty} W_{In}^a(x)\sin\beta y \\ w_{II}^a(x,y) &= \sum_{n=1}^{\infty} W_{IIn}^a(x)\sin\beta y \end{aligned} \tag{20}$$

which satisfy the simply supported plate boundary conditions at $y = 0$ and $y = b$ and where $\beta = \frac{n\pi}{b}$. Taking the deflections back into the general governing equation of plate bending problems [1] we obtain:

$$\frac{\partial^4 W_{In}^a}{\partial x^4} - 2\beta^2\frac{\partial^2 W_{In}^a}{\partial x^2} + \beta^4 W_{In}^a = \frac{Q_n}{I_1^I E_1} \tag{21}$$

where under the presence of a concentrated force with point of action located at x_0 and y_0 the function $Q_n(x)$ becomes [4]:

$$Q_n = \frac{2Q_0}{b}\delta(x - x_0)\sin\beta y_0 \tag{22}$$

For the uncracked portion of the plate there is no external load, therefore we have:

$$\frac{\partial^4 W_{IIn}^a}{\partial x^4} - 2\beta^2\frac{\partial^2 W_{IIn}^a}{\partial x^2} + \beta^4 W_{IIn}^a = 0 \tag{23}$$

The solution functions are:

$$\begin{aligned} W_{In}^a(x) = {} & A_{1n}e^{\beta x} + A_{2n}e^{\beta x}\cdot x + A_{3n}e^{-\beta x} \\ & + A_{4n}e^{-\beta x}\cdot x \\ & + \frac{Q_0\sin\beta y_0(\beta(x-x_0)\cdot\cosh\beta(x-x_0)}{\beta^3 b I_1^I E_1} \\ & - \frac{\sinh\beta(x-x_0)}{\beta^3 b I_1^I E_1} \end{aligned} \tag{24}$$

if $x_0 \le x \le a$, and:

$$\begin{aligned} W_{In}^a(x) = {} & A_{1n}e^{\beta x} + A_{2n}e^{\beta x}\cdot x \\ & + A_{3n}e^{-\beta x} + A_{4n}e^{-\beta x}\cdot x \end{aligned} \tag{25}$$

if $0 \le x \le x_0$, moreover:

$$\begin{aligned} W_{IIn}^a(x) = {} & B_{1n}e^{\beta x} + B_{2n}e^{\beta x}\cdot x \\ & + B_{3n}e^{-\beta x} + B_{4n}e^{-\beta x}\cdot x \end{aligned} \tag{26}$$

if $-c \le x \le 0$. In the solutions above A_{in} and B_{in} are constants and the subscript n refers to the number of actual Fourier term. The solution functions must satisfy the following boundary conditions:

$$W_{In}^a(a) = 0, \qquad \left.\frac{\partial^2 W_{In}^a}{\partial x^2} - \beta^2\nu W_{In}^a\right|_{x=a} = 0 \tag{27}$$

$$W_{IIn}^a(-c) = 0$$

$$\left.\frac{\partial^2 W_{IIn}^a}{\partial x^2} - \beta^2\nu W_{IIn}^a\right|_{x=-c} = 0 \tag{28}$$

Moreover, continuity of the deflection, slope, bending moment and effective (Kirchhoff) shear force must be ensured involving the following conditions [68, 69]:

$$\begin{aligned} &W_{In}^a(0) = W_{IIn}^a(0) \\ &\left.\frac{\partial W_{In}^a}{\partial x}\right|_{x=0} = \left.\frac{\partial W_{IIn}^a}{\partial x}\right|_{x=0} \end{aligned} \tag{29}$$

$$I_1^I\left(\frac{\partial^2 W_{In}^a}{\partial x^2}-\beta^2\nu W_{In}^a\right)\Big|_{x=0}$$
$$=I_1^{II}\left(\frac{\partial^2 W_{IIn}^a}{\partial x^2}-\beta^2\nu W_{IIn}^a\right)\Big|_{x=0} \tag{30}$$
$$I_1^I\left(\frac{\partial^3 W_{In}^a}{\partial x^3}-\beta^2(2-\nu)\frac{\partial W_{In}^a}{\partial x}\right)\Big|_{x=0}$$
$$=I_1^{II}\left(\frac{\partial^3 W_{IIn}^a}{\partial x^3}-\beta^2(2-\nu)\frac{\partial W_{IIn}^a}{\partial x}\right)\Big|_{x=0} \tag{31}$$

Using the above conditions and the deflection functions the eight unknown constants and the deflection functions can be calculated. Essentially, based on problem (a) it is possible to calculate the interface shear stress, τ_{xz} along the crack front. The shear forces can be expressed as [1, 2]:

$$Q_x=-I_1^{II}E_1(\triangle w)_{,x}$$
$$Q_y=-I_1^{II}E_1(\triangle w)_{,y} \tag{32}$$

Accordingly, the transverse shear stresses in the interface plane of the uncracked part are given by:

$$\tau_{xz}^0(x,y)$$
$$=\left(\frac{3}{2}\frac{Q_x(x,y)}{t}\right)$$
$$=-\frac{3I_1^{II}}{2t}\sum_{n=1}^{\infty}\left(\frac{\partial^3 W_{IIn}^a}{\partial x^3}-\beta^2\frac{\partial W_{IIn}^a}{\partial x}\right)\sin\beta y$$
$$=\sum_{n=1}^{\infty}T_n^0(x)\sin\beta y \tag{33}$$
$$\tau_{yz}^0(x,y)$$
$$=\left(\frac{3}{2}\frac{Q_y(x,y)}{t}\right)$$
$$=-\frac{3I_1^{II}}{2t}\sum_{n=1}^{\infty}\left(\beta\frac{\partial^2 W_{IIn}^a}{\partial x^2}-\beta^3 W_{IIn}^a\right)\cos\beta y$$
$$=\sum_{n=1}^{\infty}R_n^0(x)\cos\beta y \tag{34}$$

4.2 Problem (b)—simply supported plate subject to shear tractions

In accordance with Eqs. (33)–(34) it is reasonable to approximate the interface shear stresses in the form of:

$$\tau_{xz}(x,y)=\sum_{n=1}^{\infty}T_n(x)\sin\beta y$$
$$\tau_{yz}(x,y)=\sum_{n=1}^{\infty}R_n(x)\cos\beta y \tag{35}$$

i.e., similarly to the deflections the shear stresses are approximated by Fourier series in the y direction. Taking the shear stress solutions back into the governing equations (Eqs. (16)–(17)) one can obtain:

$$\frac{\partial^4 T_n(x)}{\partial x^4}-S_1\frac{\partial^2 T_n(x)}{\partial x^2}+S_2T_n(x)=0$$
$$\frac{\partial^4 R_n(x)}{\partial x^4}-S_1\frac{\partial^2 R_n(x)}{\partial x^2}+S_2R_n(x)=0 \tag{36}$$

where: $S_1=A+B\beta^2$, $S_2=\beta^4+A\beta^2+C$. The solution can be found in the form of exponential functions. The characteristic roots of Eq. (36) using Eq. (18) are:

$$\lambda_1=-\sqrt{\frac{3(1-\nu)}{8t^2}+\left(\frac{n\pi}{b}\right)^2}$$
$$\lambda_2=\sqrt{\frac{3(1-\nu)}{8t^2}+\left(\frac{n\pi}{b}\right)^2}$$
$$\lambda_3=-\sqrt{\frac{3}{4t^2}+\left(\frac{n\pi}{b}\right)^2} \tag{37}$$
$$\lambda_4=\sqrt{\frac{3}{4t^2}+\left(\frac{n\pi}{b}\right)^2}$$

The solution functions are:

$$T_n(x)=\sum_{i=1}^{4}C_{in}e^{\lambda_i x},\qquad R_n(x)=\sum_{i=1}^{4}D_{in}e^{\lambda_i x} \tag{38}$$

Eq. (38) contains eight unknown coefficients. However, the shear stresses must satisfy the coupled governing equation. Taking back Eq. (38) into (15) the relationship between C_{in} and D_{in} can be established:

$$D_{in}=\frac{2\lambda_i^2-(1-\nu)(\beta^2+3/4t^2)}{\lambda_i\beta(1+\nu)}C_{in}$$
$$D_{in}=\frac{\lambda_i\beta(1+\nu)}{2\beta^2-(1-\nu)(\lambda_i^2-3/4t^2)}C_{in} \tag{39}$$

i.e., C_{in} and D_{in} are not independent of each other, and if λ_i is a characteristic root, then both equations in (39) have to give the same. Based on the equilibrium equations (Eq. (1)) and the interface shear stresses the in-plane shear force can be expressed as:

$$N_{xy}(x,y) = \sum_{n=1}^{\infty} n_{nxy}(x) \cdot \cos \beta y \tag{40}$$

Investigating the compatibility condition given by Eq. (14) yields:

$$\frac{\partial^4 n_{nxy}}{\partial x^4} - 2\beta^2 \frac{\partial^2 n_{nxy}}{\partial x^2} + \beta^4 n_{nxy} = \beta^3 T_n - \frac{\partial^3 R_n}{\partial x^3} + \nu\left(\beta \frac{\partial^2 T_n}{\partial x^2} - \beta^2 \frac{\partial R_n}{\partial x}\right) \tag{41}$$

The homogeneous and particular solutions of n_{nxy} are:

$$n^h_{nxy}(x) = K_{1n}e^{\beta x} + K_{2n}e^{\beta x} \cdot x + K_{3n}e^{-\beta x} + K_{4n}e^{-\beta x} \cdot x \tag{42}$$

$$n^p_{nxy}(x) = \sum_{i=1}^{4} C_i \frac{\beta e^{\lambda_i}(\nu\lambda_i^2 + \beta^2)}{(\beta^2 - \lambda_i^2)^2} - \sum_{i=1}^{4} D_i \frac{\lambda_i e^{\lambda_i}(\lambda_i^2 + \nu\beta^2)}{(\beta^2 - \lambda_i^2)^2} \tag{43}$$

It can be shown by taking back Eqs. (43), (38) and (49) (see later) into Eq. (10) that the compatibility condition can be satisfied only by λ_1 and λ_2. Consequently, due to this condition and Eq. (39) we have: $C_3 = C_4 = D_3 = D_4 = 0$. As a next step we formulate the deflection functions for problem (b). The plate is still simply supported, therefore:

$$w^b_I(x,y) = \sum_{n=1}^{\infty} W^b_{In}(x) \sin \beta y$$
$$w^b_{II}(x,y) = \sum_{n=1}^{\infty} W^b_{IIn}(x) \sin \beta y \tag{44}$$

where the superscript b refers to problem (b). Substituting the deflections into the plate equation (left-hand side of Eq. (11)) we have the following equations for the delaminated and uncracked portions, respectively:

$$\frac{\partial^4 W^b_{In}(x)}{\partial x^4} - 2\beta^2 \frac{\partial^2 W^b_{In}(x)}{\partial x^2} + \beta^4 W^b_{In}(x) = 0 \tag{45}$$

$$\frac{\partial^4 W^b_{IIn}(x)}{\partial x^4} - 2\beta^2 \frac{\partial^2 W^b_{IIn}(x)}{\partial x^2} + \beta^4 W^b_{IIn}(x) = \frac{t}{2I_1^I E_1}\left(\frac{\partial T_n(x)}{\partial x} - \beta R_n(x)\right) = \frac{t}{2I_1^I E_1}\sum_{i=1}^{4}\left(\lambda_i C_{in} e^{\lambda_i x} - \beta D_{in} e^{\lambda_i x}\right) \tag{46}$$

Note, that we consider only one half of the problem, due to symmetry with respect to the x axis. This is the reason for applying $I_1 = I_1^{II}/2$ in Eq. (11). The solutions are given by:

$$W^b_{In}(x) = G_{1n}e^{\beta x} + G_{2n}e^{\beta x} \cdot x + G_{3n}e^{-\beta x} + G_{4n}e^{-\beta x} \cdot x \tag{47}$$

$$W^b_{IIn}(x) = H_{1n}e^{\beta x} + H_{2n}e^{\beta x} \cdot x + H_{3n}e^{-\beta x} + H_{4n}e^{-\beta x} \cdot x + W^b_{IInp}(x) \tag{48}$$

where $W^b_{IInp}(x)$ is the particular solution of Eq. (46) (uncracked portion):

$$W^b_{IInp}(x) = \frac{t}{I_1^{II} E_1}\left\{\sum_{i=1}^{4} C_i \frac{\lambda_i e^{\lambda_i}}{(\beta^2 - \lambda_i^2)^2} - \sum_{i=1}^{4} D_i \frac{\beta e^{\lambda_i}}{(\beta^2 - \lambda_i^2)^2}\right\} \tag{49}$$

Eqs. (38), (47) and (48) contain 10 independent constants. The four boundary and four continuity conditions are the same as those for problem (a), see Eqs. (27)–(31). Two more conditions can be formulated with respect to the shear stresses. The shear stress, τ_{xz} must vanish at the end of the uncracked portion, therefore we have:

$$T_n(-c) = 0 \tag{50}$$

The former involves that τ_{yz} (or R_n) decays also to zero. The last condition is obtained based on the axial equilibrium of the resultant forces obtained from the shear tractions along the midplanes of the cracked and uncracked portions [22]. However, in this respect we need to use two conditions. First, we assume that in the y direction the distribution of τ_{xz} in problem (b) is the same as that in problem (a). For that we utilize the following:

$$\tau_{xz}^{(a)}\big|_{z=0} = \sum_{n=1}^{\infty} T_n^0(x)\sin\beta y \tag{51}$$

where $\tau_{xz}^{(a)}$ is the shear stress in the midplane of the uncracked part using Eq. (33) for problem (a). Then, the tenth condition is:

$$T_n(0) = CT_n^0(x) \tag{52}$$

where C is determined by the axial equilibrium of the shear tractions in the midplanes of regions I and II, respectively (refer to Fig. 5):

$$\int_0^b\int_{x_0}^a \tau_{xz}^{(a)}\Big|_{z=-t/2} dxdy + \int_0^b\int_0^{x_0} \tau_{xz}^{(a)}\Big|_{z=-t/2} dxdy - \int_0^b\int_{-c}^0 \tau_{xz} dxdy = 0 \tag{53}$$

where $\tau_{xz}^{(a)}$ is the shear stress in the $z=-t/2$ plane (interface plane), refer to Eq. (7) in the delaminated region from problem (a), while τ_{xz} is the interfacial shear stress in problem (b). We note that in the y direction the equilibrium of shear tractions is also satisfied (see later the asymmetric distribution of τ_{yz}). Finally, by taking back Eqs. (38), (42), (43), (48) and (49) into (10) it can be seen that K_{in} and H_{in} constants are not independent of each other, the relationships among them are:

$$\begin{aligned} K_{1n} &= -Gt^2\beta(\beta H_{1n} + H_{2n}) \\ K_{2n} &= -Gt^2\beta^2 H_{2n} \\ K_{3n} &= Gt^2\beta(\beta H_{3n} - H_{2n}) \\ K_{4n} &= Gt^2\beta^2 H_{4n} \end{aligned} \tag{54}$$

That means ten constants and ten conditions, consequently the system of equations can be solved. Based on the deflection functions it is possible to calculate the in-plane forces and interface stresses by substituting back the constants (C_{in} and D_{in}) into Eq. (38) and utilizing the equilibrium equations (Eq. (1)). The ERR calculation is detailed in the next section.

5 Determination of the energy release rate and mode mixity

It is well-known that for a linear elastic homogeneous material the J-integral is equivalent to the ERR. In the general 3D case the J-integral is [49, 50, 70]:

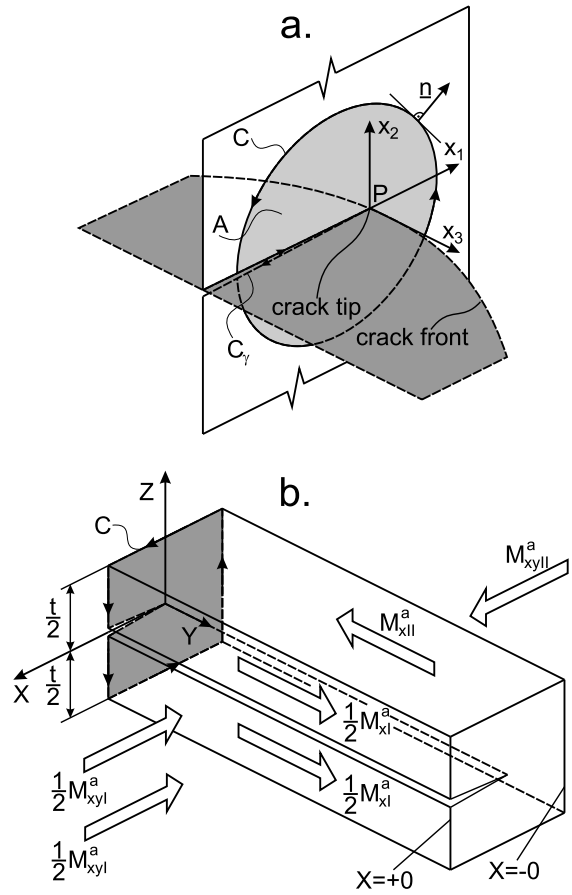

Fig. 6 Integration path for the 3-dimensional J-integral (**a**) and reference system for problem a (**b**)

$$J_k = \int_C (Wn_k - \sigma_{ij}u_{i,k}n_j)ds + \int_A (W\delta_{k3} - \sigma_{i3}u_{i,k})_{,3}dA \tag{55}$$

where $k = 1, 2$ and:

$$J_3 = \int_C (W_3 n_1 - \sigma_{3j}u_{3,1}n_j)ds \tag{56}$$

where W and W_3 are the strain energy densities:

$$W = \int_0^{\varepsilon_{ij}} \sigma_{ij}d\varepsilon_{ij}, \qquad W_3 = \int_0^{\varepsilon_{3j}} \sigma_{3j}d\varepsilon_{3j} \tag{57}$$

where according to Fig. 6a n_k is the outward normal vector of the contour C, δ_{ij} is the Kronecker tensor, σ_{ij} is the stress tensor ($\sigma_{ij}n_j$ is the traction vector),

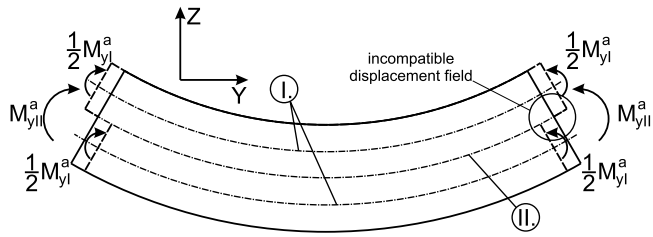

Fig. 7 Incompatible displacement field predicted by Kirchhoff plate theory

u_i is the displacement vector, A is the area enclosed by contour C. The contour C contains the crack tip and the integration is carried out in the counterclockwise direction (see Fig. 6a). To separate the mixed mode J-integral including all of the three fracture modes there is a direct method (see e.g. [49, 50]) based on the J_k integrals:

$$J_1 = J_I + J_{II} + J_{III}, \qquad J_2 = -2\sqrt{J_I J_{II}}$$
$$J_3 = J_{III} \tag{58}$$

i.e., in the general case the J_{III} integral is directly obtained from J_3. The above method is relatively simple, however in certain cases the integration of singular functions can lead to erroneous results. An other decomposition method has been proposed by Shivakumar and Raju [49] which is based on the separation of the displacement and stress components into symmetric and antisymmetric parts. Later, it was shown by Rigby and Aliabadi [50] that the stress decomposition in [49] was partly incorrect and the method has been revisited, which was applied later by numerous authors, e.g.: [52, 71].

In our case $x_1 = x$, $x_2 = z$ and $x_3 = y$ (refer to Figs. 6a–b). For the calculation we apply a zero-area path [61], in other words the integration bounds are $x = -0$ and $x = +0$ around the crack tip, which is shown by Fig. 6b. This way the surface integral in Eq. (55) becomes zero.

5.1 J-integral for problem (a)

For problem (a) the strain energy density becomes:

$$W = \frac{1}{2}(\sigma_x \varepsilon_x + \sigma_y \varepsilon_y + \tau_{xy}\gamma_{xy}) \tag{59}$$

where:

$$\begin{bmatrix} \sigma_x \\ \sigma_y \\ \tau_{xy} \end{bmatrix} = \frac{z}{I_1} \begin{bmatrix} M_x \\ M_y \\ M_{xy} \end{bmatrix}$$
$$\begin{bmatrix} \varepsilon_x \\ \varepsilon_y \\ \gamma_{xy} \end{bmatrix} = -z \begin{bmatrix} w_{,xx} \\ w_{,yy} \\ 2w_{,xy} \end{bmatrix} \tag{60}$$

In the above expression the terms related to σ_y and ε_y in J_1 and J_3 should be ignored. This can be justified by the incompatible displacement field illustrated in Fig. 7. Theoretically, if there is no crack opening, then at the point where the cracked and uncracked parts are connected to each other the strain in the y direction and the distribution of the stress σ_y are the same, in other words there is no discontinuity in this respect. Therefore, in the ideal case the integration of the stress, σ_y producted by the strain in the y direction along contour C would lead to zero. Consequently, the Kirchhoff plate model predicts erroneously the stress state in the transition zone, which can be counteracted only by ignoring the terms in question. Thus, the J-integrals for problem (a) are:

$$J_{1a} = -\frac{1}{2}\left(M^a_{xI} w^a_{I,xx}\big|_{x=+0} - M^a_{xII} w^a_{II,xx}\big|_{x=-0}\right) + 2\left(M^a_{xyI} w^a_{I,xy}\big|_{x=+0} - M^a_{xyII} w^a_{II,xy}\big|_{x=-0}\right) \tag{61}$$

$$J_{2a} = 0$$
$$J_{3a} = 2\left(M^a_{xyI} w^a_{I,xy}\big|_{x=+0} - M^a_{xyII} w^a_{II,xy}\big|_{x=-0}\right) \tag{62}$$

Based on the direct decomposition method (Eq. (58)), we have:

$$J_{IIa}(y) = -\frac{1}{2}\big(M^a_{xI} w^a_{I,xx}\big|_{x=+0} - M^a_{xII} w^a_{II,xx}\big|_{x=-0}\big)$$
$$J_{IIIa}(y) = 2\big(M^a_{xyI} w^a_{I,xy}\big|_{x=+0} - M^a_{xyII} w^a_{II,xy}\big|_{x=-0}\big) \tag{63}$$

5.2 J-integral for problem (b)

For problem (b) the strain energy densities are:

$$W^I = \frac{1}{2}\big(\sigma^I_x \varepsilon^I_x + \sigma^I_y \varepsilon^I_y + \tau^I_{xy}\gamma^I_{xy}\big)$$
$$W^I_3 = \frac{1}{2}\big(\sigma^I_y \varepsilon^I_y + \tau^I_{xy}\gamma^I_{xy}\big)$$
$$W^{II} = \frac{1}{2}\big(\sigma^{II}_x \varepsilon^{II}_x + \sigma^{II}_y \varepsilon^{II}_y + \tau^{II}_{xy}\gamma^{II}_{xy} + \tau^{II}_{xz}\gamma^{II}_{zy} + \tau^{II}_{yz}\gamma^{II}_{yz}\big) \tag{64}$$
$$W^{II}_3 = \frac{1}{2}\big(\sigma^{II}_y \varepsilon^{II}_y + \tau^{II}_{xy}\gamma^{II}_{xy} + \tau^{II}_{yz}\gamma^{II}_{yz}\big)$$

where "I" refers to the delaminated part, "II" refers to the uncracked part of the plate, τ_{xz} and τ_{yz} are given by Eqs. (7), moreover $\gamma_{xz} = \tau_{xz}/G$ and $\gamma_{yz} = \tau_{yz}/G$. For the delaminated part the J-integral is calculated in the same way as that for problem (a) using Eq. (60). In contrast, for the uncracked part the stresses are:

$$\sigma^{II}_x = E_1\big(\varepsilon^{II}_x + \nu\varepsilon^{II}_y\big)$$
$$\sigma^{II}_y = E_1\big(\varepsilon^{II}_y + \nu\varepsilon^{II}_x\big) \tag{65}$$
$$\tau^{II}_{xy} = G\gamma^{II}_{xy}$$

where ε_x, ε_y and γ_{xy} can be calculated by Eq. (60). Thus, we have:

$$J_{1b} = -\int_{-t/2}^{t/2} W^I dz + \int_{-t/2}^{t/2} \big(\sigma^I_x \varepsilon^I_x + \tau^I_{yx}\gamma^I_{xy}\big)dz + \int_{-t/2}^{t/2} W^{II} dz - \int_{-t/2}^{t/2} \left(\sigma^{II}_x \frac{\partial u_{II}}{\partial x} + \tau^{II}_{yx}\frac{\partial v_{II}}{\partial x} + \tau^{II}_{zx}\frac{\partial w_{II}}{\partial x}\right)dz \tag{66}$$

where $\varepsilon^I_x = w_{I,xx}\cdot z$, $\gamma^I_{xy} = 2\cdot w_{I,xy}\cdot z$, furthermore u_{II}, v_{II} are given by:

$$u_{II} = u_{0II} - \frac{\partial w_{II}}{\partial x}z, \qquad v_{II} = v_{0II} - \frac{\partial w_{II}}{\partial y}z \tag{67}$$

where u_0 and v_0 can be determined based on Eqs. (5), while w_{II} is given by the second of Eq. (44). Similarly to problem (a), $J_{2b} = 0$, moreover:

$$J_{3b} = -\int_{-t/2}^{t/2} W^I_3 dz + \int_{-t/2}^{t/2} \tau^I_{yx}\frac{\partial v_I}{\partial x}dz + \int_{-t/2}^{t/2} W^{II}_3 dz - \int_{-t/2}^{t/2} \tau^{II}_{yx}\frac{\partial v_{II}}{\partial x}dz \tag{68}$$

Again, the terms related to σ_y and ε_y in J_{1b} and J_{3b} should be ignored. Although displacement and shear strain continuity is ensured for the uncracked portion, for the delaminated part it is not. Calculating the mode-II and mode-III integrals we have: $J_{IIb} = 2\cdot J_{1b} - 2\cdot J_{3b}$ and $J_{IIIb} = 2\cdot J_{3b}$ where a production by 2 is necessary because we have two layers (top and bottom), and for problem (b) only one of them have been analyzed. Thus, we obtain:

$$J_{IIb} = 2\left\{-\frac{1}{2}\big(M_{xI} w_{I,xx}|_{x=+0} - M_{xII} w_{II,xx}|_{x=-0}\big) + \frac{1}{2}N_x \varepsilon^0_x\Big|_{x=-0} + \int_{-t/2}^{t/2} \tau_{xz}\left(w_{II,x} - \frac{1}{2}u_{II,z}\right)dz\Big|_{x=-0}\right\} \tag{69}$$

$$J_{IIIb} = 2\left\{2\big(M^b_{xyI} w^b_{I,xy}\big|_{x=+0} - M^b_{xyII} w^b_{II,xy}\big|_{x=-0}\big) + N_{xy}\left(\frac{1}{2}\gamma^0_{xy} + v^b_{II,x}\right)\Big|_{x=-0} - \frac{1}{2}\int_{t/2}^{t/2} \tau_{yz} v^b_{II,z} dz\Big|_{x=-0}\right\} \tag{70}$$

where based on Eq. (6):

$$u_{II,z} = k_{sh}\frac{\partial \tau_{xz}}{\partial z}, \qquad v_{II,z} = k_{sh}\frac{\partial \tau_{yz}}{\partial z} \tag{71}$$

Table 1 The convergence of the plate theory solution by increasing the number of Fourier terms

N	1	3	5	7	9	11	13	15	17	19
$w_I^a(x_0, y_0)$ [mm]	−4.883	−5.146	−5.205	−5.226	−5.236	−5.241	−5.245	−5.247	−5.248	−5.249
$N_x(0, b/2)$ [N/mm]	−13.15	−14.30	−14.42	−14.44	−14.44	−14.44	−14.44	−14.44	−14.44	−14.43
$N_{xy}(0, 0)$ [N/mm]	4.91	4.77	4.78	4.78	4.78	4.78	4.78	4.78	4.78	4.78
$\tau_{xz}(0, b/2)$ [N/mm^2]	−1.466	−1.689	−1.1720	−1.7249	−1.7255	−1.7256	−1.7256	−1.7256	−1.7256	−1.7256
$\tau_{yz}(0, 0)$ [N/mm^2]	−0.1358	−0.0760	−0.0894	−0.0869	−0.0873	−0.0873	−0.0873	−0.0873	−0.0873	−0.0873
$G_{II}(0, b/2)$ [J/m^2]	64.6	91.7	96.3	97.0	97.1	97.1	97.1	97.1	97.1	97.1
$G_{III}(0, 0)$ [J/m^2]	517.4	403.2	418.1	416.0	416.3	416.3	416.3	416.3	416.3	416.3

Finally, the ERRs are:

$$G_{II} = J_{II} = J_{IIa} + J_{IIb}$$
$$G_{III} = J_{III} = J_{IIIa} + J_{IIIb} \tag{72}$$

The mode mixity (G_{II}/G_{III}) is calculated by using Eq. (72) at each y location along the crack front.

6 Results and discussion

The properties of the analyzed simply supported plate were (refer to Fig. 4): $a = 105$ mm (crack length), $c = 45$ mm (uncracked length), $b = 100$ mm (plate width), $t = 1.55$ mm (plate thickness), $E = 33$ GPa (modulus of elasticity), $\nu = 0.27$ (Poisson's ratio), $Q_0 = 1000$ N (point force magnitude), $x_0 = 31$ mm, $y_0 = 50$ mm (point of action coordinates of Q_0). The computation was performed by using the code MAPLE [72] in accordance with the following points. First, problem (a) in Fig. 4 was solved varying the number of Fourier series terms (N) by creating a for-do cycle. Then, from the deflection functions of problem (a) the transverse shear stress was calculated (Eq. (33)). The next step was the solution of problem (b) in Fig. 5, the system of equations was constructed using Eqs. (38), (46), (47) and (48) by utilizing the B.C.s given by Eqs. (27)–(31) and (50)–(53). The in-plane normal and shear forces were determined from Eqs. (54), (42), (43), then by using Eq. (1) while the ERRs were calculated using the J-integral.

6.1 Convergence analysis

Table 1 shows how the results converge as we increase the number of terms in the Fourier series solution. It is seen that after the 15th term there is no change in any of the quantities presented in Table 1. Consequently, the relatively fast convergence of Lévy's method [1] can be exploited also for the calculation of ERRs.

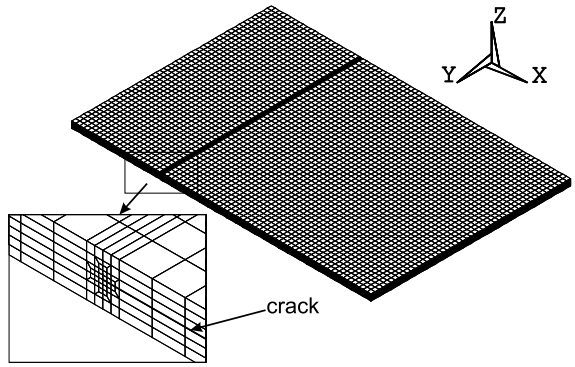

Fig. 8 ANSYS FE model of the simply supported delaminated plate

6.2 Finite element model—VCCT and J-integral

In order to verify the analytical results a finite element analysis was carried out. The 3D finite element model of the plate is shown by Fig. 8. The model was created in the commercial ANSYS 12 package using 8 node solid elements. In the vicinity of the crack tip a refined mesh was constructed including trapezoid shape elements [73]. The z displacements of contact nodes over the delaminated surface were imposed to be the same. The mode-II and mode-III ERRs were calculated by the VCCT method, the size of the crack tip elements were $\Delta x = 0.25$ mm, $\Delta y = 0.25$ mm and $\Delta z = 2$ mm. For the determination of G_{II} and G_{III} a so-called MACRO was written in the ANSYS Design and Parametric Language (ADPL). The MACRO gets the nodal forces and displacements at the crack tip and at each pair of nodes, respectively, then by

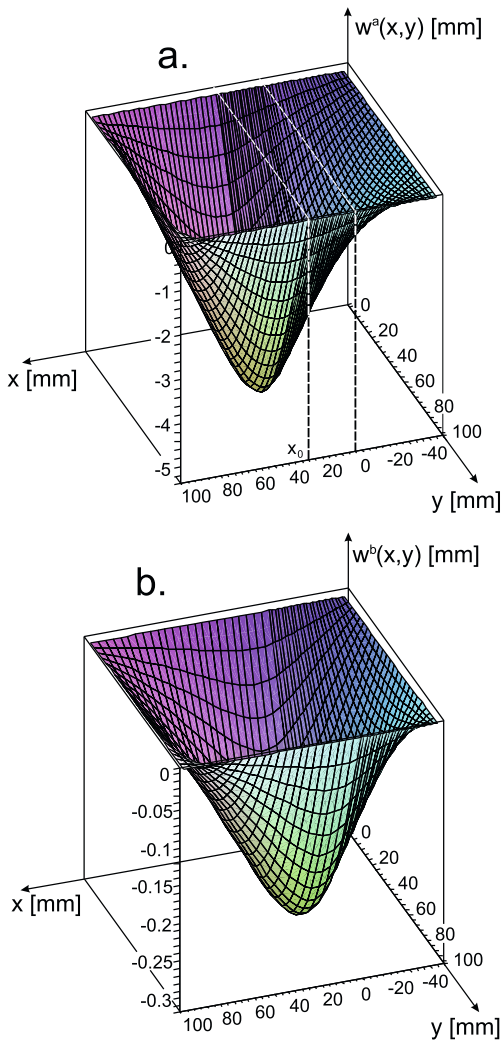

Fig. 9 Plate deflections from subproblems (**a**) and (**b**)

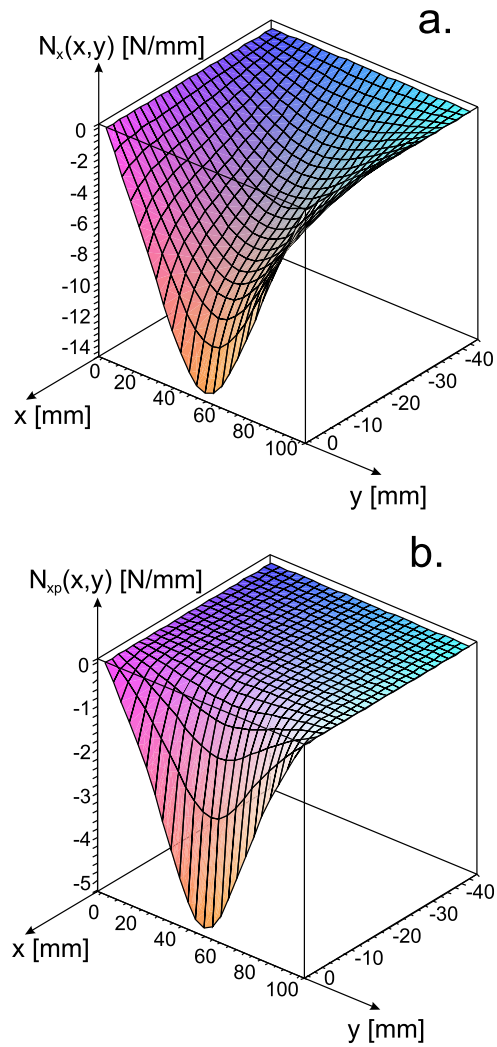

Fig. 10 Distribution of total (**a**) and particular (**b**) solutions of the in-plane normal force

defining the size of crack tip elements it determines and plots the ERRs at each point along the crack front. Apart from the VCCT G_{II} and G_{III} were determined also by the J-integral, which is available in ANSYS 12 as a built-in command.

6.3 Kirchhoff plate theory results

The deflection functions calculated for problems (a) and (b) are depicted in Fig. 9, respectively when $N = 19$ (number of terms in the Fourier series). As expected, the maximum deflection in problem (a) takes place at the point of action of Q_0. Compared to problem (a), problem (b) provides essentially very small displacement values.

Figures 10 and 11 demonstrate the distribution of the in-plane normal and shear forces over the interface of the undelaminated region of the top plate ($N = 19$). The total solutions are shown by Figs. 10a and 11a. For N_x the total solution vanishes only at the end of the plate, while N_{xp} decays very fastly behind the crack front. Similar conclusions can be drawn based on Figs. 11a and 11b. It is important to note that the homogeneous part of N_{xy} is induced by the twisting curvature of the top and bottom plate elements (refer to Fig. 3b), while the particular solution is related to the interface shear stresses.

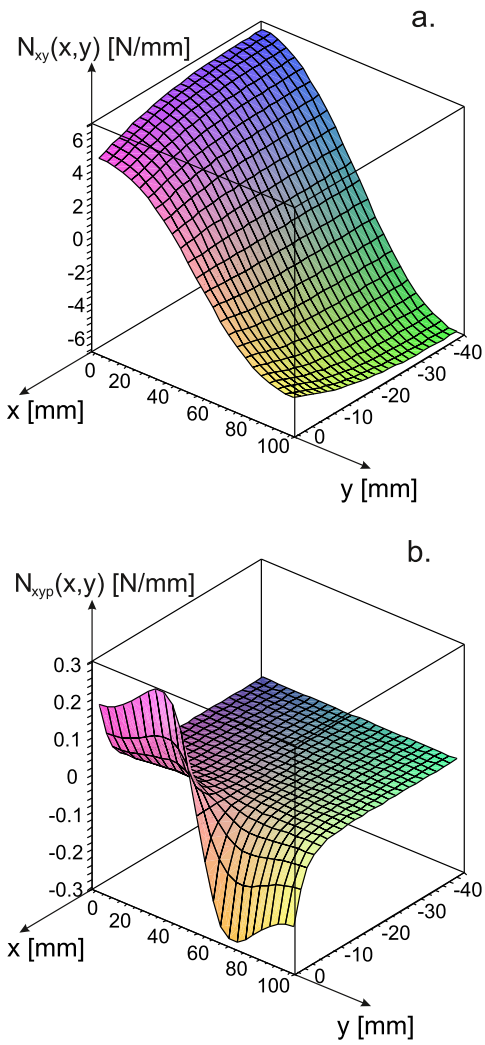

Fig. 11 Distribution of total (**a**) and particular (**b**) solutions of the in-plane shear force

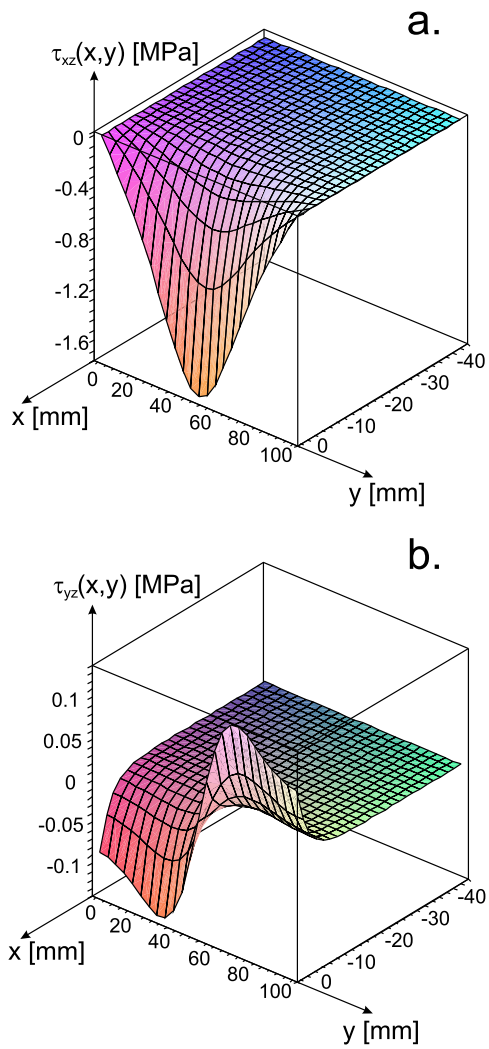

Fig. 12 Distribution of the interface shear stresses: τ_{xz} (**a**), τ_{yz} (**b**)

The interface shear stresses are plotted in Fig. 12. Similarly to the particular solution of in-plane forces, they decay fastly to zero behind the crack front.

The mode-II, mode-III ERRs and the mode ratio along the crack front are shown by Fig. 13. The symbols show the result of the VCCT and the J-integral by FEM, while the curves represent the purely analytical plate theory solutions. The solution of problem (a) provides the major part of the ERRs. It is seen that the mode-II component is significantly underestimated by the classical plate theory solution. On the contrary the mode-III component is overestimated. Problem (b) provides a reasonable improvement for the mode-II ERR, which is 43.8 % for G_{II} and only -5.7 % for G_{III}.

Also, it is clear that plate theory still underestimates the mode-II component, in the midpoint the difference is about 24.5 % compared to the VCCT result. In contrast, the mode-III ERR is slightly smaller compared to the plate theory. From this point of view the difference between maximum of the mode-III ERR by VCCT and the plate model is about 1.2 %. While the VCCT predicts that the mode-III ERR decays suddenly near the edges, there is not any decay in accordance with the plate solution. From the practical point of view this difference is insignificant. The crack is expected to initiate/propagate at the points where the highest ERR

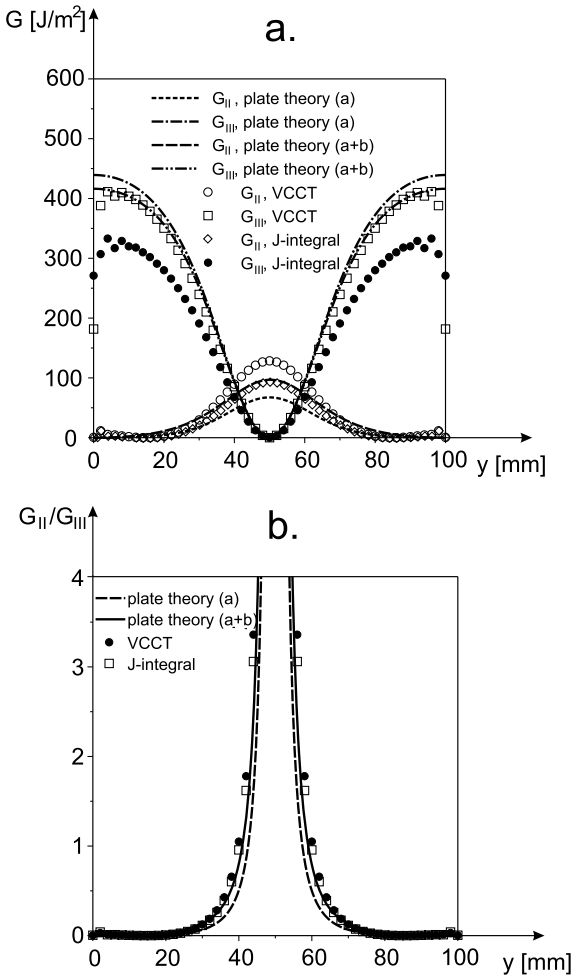

Fig. 13 Energy release rate distributions (**a**) and mode ratios (**b**) by Kirchhoff plate theory (Lévy solution) and FE analysis (VCCT and J-integral)

takes place. This point is in fact almost identical predicted by the two methods. The ANSYS' J-integral underpredicts both ERR components in comparison with the VCCT. In this respect, the plate theory solution $(a+b)$ agrees very-well with the mode-II ERR, on the contrary the mode-III component by the numerical J-integral is significantly underpredicted and neither the plate theory nor the VCCT shows good agreement with it.

The mode ratio (G_{II}/G_{III}) is depicted in Fig. 13b. It shows that the VCCT and the numerical J-integral is in a reasonably good agreement with each other. The classical plate theory solution (a) slightly underestimates the mode ratio, however the contribution of problem (b) makes the solution matching well with the numerical results.

The overall agreement between the VCCT and plate theory methods is fairly good. The difference between the VCCT and plate theory solution can be attributed to the transverse shear effect. Moreover, the continuity of the displacements is ensured only in problem (b), and it was elaborated that the stress and displacement fields in the y direction lead to incompatibilities in problem (a).

It has been shown in numerous papers that transverse shear has a significant effect on the ERRs [24, 26, 56, 57]. It is expected that in the case of the mode-II ERR the effect of transverse shear takes place in higher degree in the middle of the crack front, while it vanishes at the plate edges. Considering the mode-III ERR the transverse shear effect is assumed to be significant near the edges and negligible in the middle of the crack front.

7 Applications, future developments

The possible application field of the presented method is the fracture mechanics of composite materials. In the last few years test methods involving the bending of delaminated composite plates have been developed [17, 33, 39] for mode-III, mixed-mode II/III and I/III. For the determination of the ERR an analytical data reduction scheme has not yet been developed for these systems.

The solution can be improved by using the Reissner-Mindlin [2–4] and other higher order plate theories [74–76] to elaborate the significance of transverse shear effect on the ERRs. An essential requirement is that the formulation should be generalized for unsymmetrically delaminated plates too. Furthermore for composites the formulation should be done incorporating the theory of laminated plates. It should be noted that in the case when the top and bottom plate elements have different material properties then the shear stresses can not be expressed in the way shown in Sect. 3. A useful alternative in this case is that we derive first the governing equations of the in-plane forces, N_x and N_y, afterwards incorporating the compatibility and equilibrium equations it is possible to obtain N_{xy} and the interface shear stresses. The relevant equations are presented in the Appendix for symmetric delamination and with material isotropy, for laminated plates the procedure works similarly [77].

Finally but not least, the mode-I (opening mode) ERR was not considered in this study. A possible solution for this problem is the application of elastic foundation plates [1, 78]. Further work is necessary to include all of these effects and possibilities.

8 Conclusions

A purely analytical plate theory approach has been presented to calculate the mode-II and mode-III ERR distributions along the crack front of symmetrically delaminated, isotropic plates subjected to bending. The formulation is based on the consideration of interface shear stresses and the continuity of the displacements and shear strain over the interface of a double-plate system. The governing equations have been developed for the interface shear stresses leading to fourth order partial differential equations. The relationship among the shear stresses and the well-known fourth order PDE of plate deflection has been established. The solution of system of PDEs has been presented for a simply supported delaminated plate assuming material isotropy. To solve the problem Lévy plate formulation has been adopted. The whole problem has been solved in two steps: problem (a) covered a stepped thickness plate where the transverse shear stress has been calculated and utilized as input data (initial value) for a further analysis. Problem (b) has been formulated by separating the double-plate system into two individual plates (top and bottom) assuming shear tractions over the uncracked portions of the plates. The energy release rates have been calculated using the 3-dimensional J-integral by defining a zero-area path around the crack front. The mode-II and mode-III components have been determined by a direct mode decomposition method. The results have been compared to those of a 3D finite element model and a fairly good agreement has been found. It has been shown that for the presented problem the interface shear stresses contribute significantly only to the mode-II energy release rate.

Considering the available methods for the calculation of the ERR in plates subjected to bending the first choice is in general the VCCT method. However, for a 3D FE model the computation could be lengthy, especially if the model has relatively large dimensions. Moreover in the crack tip a refined mesh should be constructed with relatively small elements compared to the global element size to obtain accurate ERR values and reach the desired convergence. Finally, to process the FE results a user-defined subroutine is necessary, because in most of the commercial FE packages the VCCT has not yet been implemented. The other alternatives available in the literature have similar drawbacks. In this respect the present work provides another possibility for plate bending problems including delamination. The main goal of this paper is that it has been shown how we can use plate theories to predict ERR distributions in plate-like structures. From other perspectives, the disadvantages of the proposed formulation are the facts that the original problem must have an analytical solution and the ERRs can be calculated in two steps. The method can be applied for plates with through the width crack and involving simple boundary conditions wherein the Lévy plate formulation can be applied. On the other hand the two level computation can be performed in the same MAPLE worksheet and the data of the model (material and geometrical properties, load position and magnitude) can be very simply varied compared to a FE model.

Acknowledgements This work was supported by the János Bolyai Research Scholarship of the Hungarian Academy of Sciences and the National Science and Research Fund (OTKA) under Grant No. T34040 (69096). This work is connected to the scientific program of the "Development of quality-oriented and harmonized R+D+I strategy and functional model at BME" project. This project is supported by the New Hungary Development Plan (Project ID: TÁMOP-4.2.1/B-09/1/KMR-2010-0002).

Appendix

To derive the governing equations for the in-plane forces N_x and N_y we express first the moments from Eqs. (3), (9) and (10):

$$\begin{aligned} M_x &= -\frac{2I_1}{t^2}N_x + \frac{2I_1E_1k_{sh}}{t} \\ &\quad\times\left(\frac{\partial^2 N_x}{\partial x^2} - (1+\nu)\frac{\partial^2 N_{xy}}{\partial x\partial y} + \nu\frac{\partial^2 N_y}{\partial y^2}\right) \\ M_y &= -\frac{2I_1}{t^2}N_y + \frac{2I_1E_1k_{sh}}{t} \\ &\quad\times\left(\frac{\partial^2 N_y}{\partial y^2} - (1+\nu)\frac{\partial^2 N_{xy}}{\partial x\partial y} + \nu\frac{\partial^2 N_x}{\partial x^2}\right) \end{aligned} \tag{73}$$

$$M_{xy} = \frac{2I_1}{t^2} N_{xy} + \frac{I_1 E_1 (1-\nu) k_{sh}}{t} \times \left(\frac{\partial^2 N_x}{\partial x \partial y} - \frac{\partial^2 N_{xy}}{\partial x^2} - \frac{\partial^2 N_{xy}}{\partial y^2} + \frac{\partial^2 N_y}{\partial x \partial y} \right) \quad (74)$$

Incorporating the equilibrium equations (Eqs. (1), (2)) and the compatibility equation (Eq. (14)) one can obtain the following coupled PDE system:

$$A_1 \frac{\partial^4 N_x}{\partial x^4} + A_2 \frac{\partial^4 N_x}{\partial x^2 \partial y^2} + A_3 \frac{\partial^2 N_x}{\partial x^2} + A_4 \frac{\partial^4 N_x}{\partial y^4} + A_5 \frac{\partial^2 N_x}{\partial y^2} + A_6 \frac{\partial^4 N_y}{\partial x^4} + A_7 \frac{\partial^4 N_y}{\partial x^2 \partial y^2} + A_8 \frac{\partial^2 N_y}{\partial x^2} + A_9 \frac{\partial^4 N_y}{\partial y^4} + A_{10} \frac{\partial^2 N_y}{\partial y^2} = 0 \quad (75)$$

$$A_1 \frac{\partial^4 N_y}{\partial y^4} + A_2 \frac{\partial^4 N_y}{\partial x^2 \partial y^2} + A_3 \frac{\partial^2 N_y}{\partial y^2} + A_4 \frac{\partial^4 N_y}{\partial x^4} + A_5 \frac{\partial^2 N_y}{\partial x^2} + A_6 \frac{\partial^4 N_x}{\partial y^4} + A_7 \frac{\partial^4 N_x}{\partial x^2 \partial y^2} + A_8 \frac{\partial^2 N_x}{\partial y^2} + A_9 \frac{\partial^4 N_x}{\partial x^4} + A_{10} \frac{\partial^2 N_x}{\partial x^2} = 0 \quad (76)$$

where the constants are:

$$A_1 = \frac{1}{9} \frac{t^3 (4 + \nu - \nu^2)}{1 - \nu^2}$$

$$A_2 = \frac{1}{9} \frac{t^3 (5 - \nu^2)}{1 - \nu^2}$$

$$A_3 = -\frac{1}{12} \frac{t(2+\nu)}{1+\nu}, \qquad A_4 = \frac{1}{9} \frac{t^3}{1+\nu}$$

$$A_5 = -\frac{1}{12} \frac{t}{1+\nu}, \qquad A_6 = \frac{1}{9} \frac{t^3 (3+\nu)}{1-\nu^2} \quad (77)$$

$$A_7 = \frac{1}{9} \frac{t^3 (3+\nu^2)}{1-\nu^2}, \qquad A_8 = A_5$$

$$A_9 = -\nu A_4, \qquad A_{10} = -\nu A_8$$

The above PDE system can be solved by using the Fourier series solutions for N_x and N_y.

References

1. Timoshenko S, Woinowsky-Krieger S (1959) Theory of plates and shells, 2nd edn. McGraw-Hill, New York, Toronto, London
2. Ventsel E, Krauthammer T (2001) Thin plates and shells—theory, analysis and applications. Dekker, New York, Basel
3. Rudolph Sz (2004) Theories and applications of plate analysis. John Wiley, Hoboken
4. Reddy JN (2004) Mechanics of laminated composite plates and shells—theory and analysis. CRC Press, Boca Raton, London, New York, Washington
5. Allen HG (1969) Analysis and design of structural sandwich panels, 1st edn. Pergamon Press, Oxford, London, Edinburgh, New York, Toronto, Sydney, Paris, Braunschweig
6. Anderson TL (2005) Fracture mechanics—fundamentals and applications, 3rd edn. CRC Press, Taylor & Francis, Boca Raton, London, New York, Singapore
7. Jumel J, Budzik MK, Shanahan MER (2011) Beam on elastic foundation with anticlastic curvature: application to analysis of mode I fracture tests. Eng Fract Mech 78(18):3253–3269
8. Yoshihara H, Satoh A (2009) Shear and crack tip deformation correction for the double cantilever beam and three-point end-notched flexure specimens for mode I and mode II fracture toughness measurement of wood. Eng Fract Mech 76(3):335–346
9. Kim S, Kim JS, Yoon H (2011) Experimental and numerical investigations of mode I delamination behaviors of woven fabric composites with carbon, Kevlar and their hybrid fibers. J Bone Miner Metab 12(2):321–329
10. Peng L, Zhang J, Zhao L, Bao R, Yang H, Fei B (2011) Mode I delamination growth of multidirectional composite laminates under fatigue loading. J Compos Mater 45(10):1077–1090
11. Brunner AJ, Flüeler P (2005) Prospects in fracture mechanics of "engineering" laminates. Eng Fract Mech 72:899–908
12. Brunner AJ, Blackman BRK, Davies P (2008) A status report on delamination resistance testing of polymer-matrix composites. Eng Fract Mech 75:2779–2794
13. Arrese A, Carbajal N, Vargas G, Mujika F (2010) A new method for determining mode II R-curve by the end-notched flexure test. Eng Fract Mech 77(1):51–70
14. Argüelles A, Viña J, Canteli AF, Bonhomme J (2011) Influence of resin type on the delamination behavior of carbon fiber reinforced composites under mode-II loading. Int J Damage Mech 20(7):963–977
15. Plain KP, Tong L (2011) An experimental study on mode I and II fracture toughness of laminates stitched with a one-sided stitching technique. Composites, Part A, Appl Sci Manuf 42(2):203–210
16. Szekrényes A (2009) Improved analysis of the modified split-cantilever beam for mode III fracture. Int J Mech Sci 51(9–10):682–693
17. de Morais AB, Pereira AB (2009) Mode III interlaminar fracture of carbon/epoxy laminates using a four-point bending plate test. Composites, Part A, Appl Sci Manuf 40(11):1741–1746
18. de Morais AB, Pereira AB, de Moura MFSF (2011) Mode III interlaminar fracture of carbon/epoxy laminates using the six-point edge crack torsion (6ECT). Composites, Part A, Appl Sci Manuf 42(11):1793–1799
19. Davidson BA, Sediles FO (2011) Mixed-mode I-II-III delamination toughness determination via a shear-torsion-bending test. Composites, Part A, Appl Sci Manuf 42(6):589–603

20. Chatterjee SN (1991) Analysis of test specimens for interlaminar mode II fracture toughness, Part 1. Elastic laminates. J Compos Mater 25:470–493
21. Bao G, Ho S, Sou Z, Fan B (1992) The role of material orthotropy in fracture specimens for composites. Int J Solids Struct 29(9):1105–1116
22. Wang J, Qiao P (2004) Novel beam analysis of end notched flexure specimen for mode-II fracture. Eng Fract Mech 71:219–231
23. Szekrényes A (2007) Improved analysis of unidirectional composite delamination specimens. Mech Mater 39:953–974
24. Li S, Wang J, Thouless MD (2004) The effects of shear on delamination in layered materials. J Mech Phys Solids 52:193–214
25. Bennati S, Colleluori M, Corigliano D, Valvo PS (2009) An enhanced beam-theory model of the asymmetric double cantilever beam (ADCB) test for composite laminates. Compos Sci Technol 69(11–12):1735–1745
26. Andrews MG, Massabò R (2007) The effects of shear and near tip deformations on energy release rate and mode mixity of edge-cracked orthotropic layers. Eng Fract Mech 74:2700–2720
27. Hsu WH, Chue C-H (2009) Mode III fracture problem of an arbitrarily oriented crack in an FGPM strip bonded to a homogeneous piezoelectric half plane. Meccanica 44:519–534
28. Chue C-H, Yeh C-N (2011) Mode III fracture problem of two arbitrarily oriented cracks located within two bonded functionally graded material strips. Meccanica 46:447–469
29. Da Silva LFM, Estevez VHC, Chavez FJP (2011) Fracture toughness of a structural adhesive under mixed mode loadings. Materialwissenschaft und Werkstofftechnik 42(5):460–470
30. Kenane M, Benmedakhene S, Azari Z (2010) Fracture and fatigue study of unidirectional glass/epoxy laminate under different mode of loading. Fatigue Fract Eng Mater Struct 33(5):285–293
31. Jumel J, Budzik MK, Shanahan MER (2011) Process zone in the single cantilever beam under transverse loading. Part I: Theoretical analysis. Theor Appl Fract Mech 56(1):7–12
32. Szekrényes A (2009) Interlaminar fracture analysis in the G_I–G_{III} plane using prestressed composite beams. Composites, Part A, Appl Sci Manuf 40(10):1621–1631
33. Pereira AB, de Morais AB (2009) Mixed-mode I + III interlaminar fracture of carbon/epoxy laminates. Composites, Part A, Appl Sci Manuf 40(4):518–523
34. Szekrényes A (2007) Delamination fracture analysis in the G_{II}–G_{III} plane using prestressed composite beams. Int J Solids Struct 44(10):3359–3378
35. Szekrényes A (2012) Interlaminar fracture analysis in the G_{II}–G_{III} plane using prestressed composite beams. Composites, Part A, Appl Sci Manuf 43(1):95–103
36. Kondo A, Sato Y, Suemasu H, Aoki Y (2011) Fracture resistance of carbon/epoxy composite laminates under mixed-mode II and III failure and its dependence on fracture morphology. Adv Compos Mater 20(5):405–418
37. Kondo A, Sato Y, Suemasu H, Gouzu K, Aoki Y (2010) Characterization of fracture resistance of carbon/epoxy composite laminates during mixed-mode II and III stable damage propagation. J Jpn Soc Compos Mater 36(5):179–188
38. Suemasu H, Kondo A, Gozu K, Aoki Y (2010) Novel test method for mixed mode II and III interlaminar fracture toughness. Adv Compos Mater 19(4):349–361
39. de Morais AB, Pereira AB (2008) Mixed mode II + III interlaminar fracture of carbon/epoxy laminates. Compos Sci Technol 68(9):2022–2027
40. Marat-Mendes RM, Freitas MM (2010) Failure criteria for mixed mode delamination in glass fibre epoxy composites. Fifteenth International Conference on Composite Structures. Compos Struct 92(9):2292–2298
41. Szekrényes A (2011) Interlaminar fracture analysis in the G_I–G_{II}–G_{III} space using prestressed composite beams. J Reinf Plast Compos 30(19):1655–1669
42. Williams JG (1988) On the calculation of energy release rates for cracked laminates. Int J Fract 36:101–119
43. Suo Z, Hutchinson JW (1990) Interface crack between two elastic layers. Int J Fract 43:1–18
44. Suo Z (1990) Delamination specimens for orthotropic materials. J Appl Mech 57:627–634
45. Davidson BD, Hu H, Schapery RA (1995) An analytical crack-tip element for layered elastic structures. J Appl Mech 62:294–305
46. Rice JR (1968) A path independent integral and the approximate analysis of strain concentration by notches and cracks. J Appl Mech 35:379–386
47. Cherepanov GP (1997) Methods of fracture mechanics: solid matter physics. Kluwer, Dordrecht, Boston, London
48. Murakami T, Sato T (1983) Three-dimensional J-integral calculations of part-through surface crack problems. Comput Struct 17(5–6):731–736
49. Shivakumar KN, Raju IS (1992) An equivalent domain integral method for three-dimensional mixed-mode fracture problems. Eng Fract Mech 42(6):935–959
50. Rigby RH, Aliabadi MH (1998) Decomposition of the mixed-mode J-integral—revisited. Int J Solids Struct 35(17):2073–2099
51. Valaire BT, Yong YW, Suhling J, Jang BZ, Zhang SQ (1990) Application of the J-integral to mixed mode fracture of orthotropic composites. Eng Fract Mech 36(3):507–514
52. Wearing JL, Ahmadi-Brooghani SY (1999) The evaluation of stress intensity factors in plate bending problems using the dual boundary element method. Eng Anal Bound Elem 23:3–19
53. Lee LJ, Tu DW (1993) J integral for delaminated composite laminates. Compos Sci Technol 47:185–192
54. Wang JTS, Huang JT (1994) Strain-energy release rate of delaminated composite plates using continuous analysis. Compos Eng 4(7):731–744
55. Bruno D, Greco F (2001) Mixed-mode delamination in plates: a refined approach. Int J Solids Struct 38:9149–9177
56. Bruno D, Greco F (2001) Delamination in composite plates: influence of shear deformability on interfacial debonding. Cem Concr Compos 23:33–45
57. Wang J, Qiao P (2004) Interface crack between two shear deformable elastic layers. J Mech Phys Solids 52:891–905
58. Bonhomme J, Argüelles A, Castrillo MA, Viña J (2010) Computational models for mode I composite fracture fail-

ure: the virtual crack closure technique versus the two-step extension method. Meccanica 45(3):297–304
59. Qiao P, Wang J (2004) Mechanics and fracture of crack tip deformable bi-material interface. Int J Solids Struct 41:7423–7444
60. Wang J, Qiao P (2004) On the energy release rate and mode mix of delaminated shear deformable composite plates. Int J Solids Struct 41:2757–2779
61. Sankar BV, Sonik V (1995) Pointwise energy release rate in delaminated plates. AIAA J 33(7):1312–1318
62. Davidson BD, Yu L, Hu H (2000) Determination of energy release rate and mode mix in three-dimensional layered structures using plate theory. Int J Fract 105:81–104
63. Park O, Sankar BV (2002) Crack-tip force method for computing energy release rate in delaminated plates. Compos Struct 55:429–434
64. Bruno D, Greco F, Lonetti P (2005) A 3D delamination modelling technique based on plate and interface theories for laminated structures. Eur J Mech A, Solids 24(1):127–149
65. Suhir E (1986) Stresses in bi-metal thermostats. J Appl Mech 53:657–660
66. Chou PC, Pagano NJ (1967) Elasticity—tensor, dyadic, and engineering approaches. Van Nostrand, Princeton, Toronto, London
67. Chatterjee SN (1991) Analysis of test specimens for interlaminar mode II fracture toughness, Part 2. J Compos Mater 25:494–511
68. Guo SJ (1997) Vibration analysis of stepped thickness plates. J Sound Vib 204(4):645–657
69. Yingshi Z (1999) Vibrations of stepped rectangular thin plates on Winkler's foundation. Appl Math Mech 20(5):568–578
70. Chiarelli M, Frediani A (1993) A computation of the three-dimensional J-integral for elastic materials with a view to applications in fracture mechanics. Eng Fract Mech 44(5):763–788
71. Hamed MA, Nosier A, Farrahi GH (2006) Separation of delamination modes in composite beams with symmetric delaminations. Mater Des 27:900–910
72. Garvan F (2002) The maple book. Chapman & Hall/CRC, Boca Raton, London, New York, Washington
73. Davidson BD, Krüger R, König M (1995) Three-dimensional analysis of center-delaminated unidirectional and multidirectional single-leg bending specimens. Compos Sci Technol 54:385–394
74. Roque CMC, Rodrigues JD, Ferreira AJM (2012) Analysis of thick plates by local radial basis functions-finite differences method. Meccanica 47:1157–1171
75. Batista M (2012) Comparison of Reissner, Mindlin and Reddy plate models with exact three dimensional solution for simply supported isotropic and transverse inextensible rectangular plate. Meccanica 47:257–268
76. Xiang S, Kang G-W, Xing B (2012, accepted) A nth-order shear deformation theory for the free vibration analysis on the isotropic plates. Meccanica. doi:10.1007/s11012-012-9563-0
77. Szekrényes A (2012) Interlaminar stresses and energy release rates for delaminated orthotropic plates. Int J Solids Struct 49:2460–2470
78. Kumar Y, Lal R (2012) Vibrations of nonhomogeneous orthotropic rectangular plates with bilinear thickness variation resting on Winkler foundation. Meccanica 47:893–915